PAPER • **OPEN ACCESS**

Seismic Analysis of Concrete Arch Dam Considering Material Failure Criterion

To cite this article: Mohammad Hajmohammadian Baghban *et al* 2021 *IOP Conf. Ser.: Mater. Sci. Eng.* **1117** 012004

View the article online for updates and enhancements.

You may also like

- Study on dynamic contact model and force transfer mechanism of hydraulic spherical keyway
Liu He, Liaojun Zhang and Xiao Cui
- Effect of Contraction Joints on Structural Behavior of Double Curvature Concrete Dam Subject to Dynamic Loading
Saleh Issa Khassaf, Aqeel Hatem Chkheiwr and Mohammed Abdulrahim Jasim
- Optimizing efforts to restore aquatic ecosystem connectivity requires thinking beyond large dams
Lee J Baumgartner, Tim Marsden, Deanna Duffy et al.

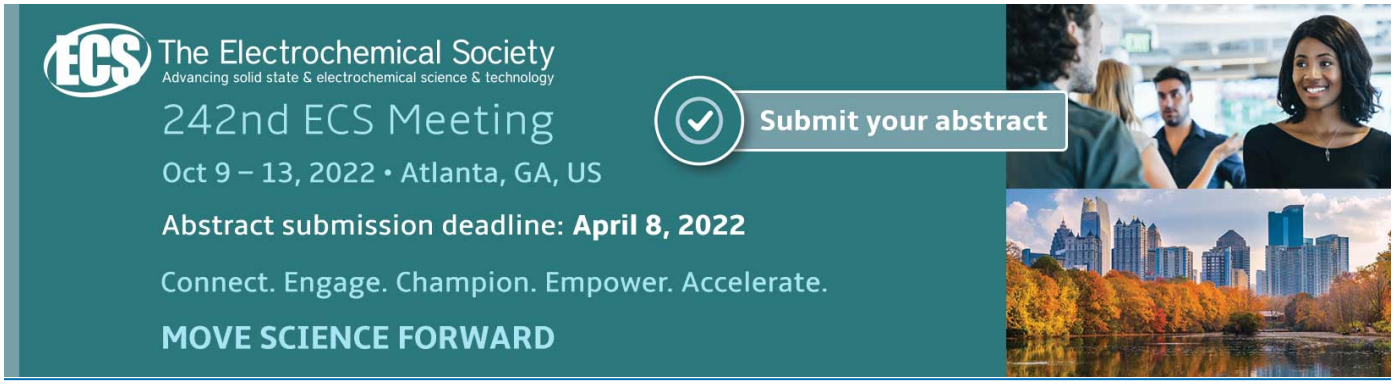

This content was downloaded from IP address 86.57.70.29 on 19/01/2022 at 20:54

Seismic Analysis of Concrete Arch Dam Considering Material Failure Criterion

Mohammad Hajmohammadian Baghban*[1], Iman Faridmehr [2], Reza Goldaran[3], Roozbeh Safaeian Amoly [3]

[1]Department of Manufacturing and Civil Engineering, Norwegian University of Science and Technology (NTNU), 2815 Gjøvik, Norway
[2] South Ural State University, 454080 Chelyabinsk, Lenin Prospect 76, Russian Federation, Russia
[3]Civil Engineering Department, Faculty of Engineering, Girne American University, Girne, N. Cyprus

*Correspondence: mohammad.baghban@ntnu.no; Tel.: +47-48-351-726

Abstract. Since large dams collapse can lead to catastrophic consequences on human's lives and properties, the reliable performance of such structures during a strong earthquake is extremely important. Therefore, applying reliable analysis methods for designing large dams and seismic evaluation of the existing dam is crucial. The present study investigates the behavior of a concrete arch dam during the maximum credible earthquake "MCL" through non-linear time history analysis. A 30-meter height concrete arch dam was simulated in SAP2000-academic version- using 3D solid elements. Rayleigh damping and plasticity-based five-parameter Willam-Warnke model, as a means of failure criterion, were taken into account during non-linear time history analysis. The results indicated that the seismic load combination had a significant impact on final stress distribution in which high tensile cracks penetrated over the upstream heel.

1. Introduction

Hydraulic structures especially large dams, have been amongst the first structures for which seismic analysis was taken into account. Being earthquake-resistant is of high importance for large dams, where collapses causing irreparable human causalities and financial losses. The majority of large dams throughout the world are located within high seismicity areas, which were affected by strong motions in the past decades. Seismic analysis of large dams is an increasing demand in engineering societies and has a great contribution to the inclusive events for seismic risk reduction. The foremost objective in seismic analysis of large dams is to facilitate understanding of the dynamic behavior and failure mechanism under seismic loading.

The seismic analysis method of large dams proposed by Westergaard in the 1930s [1] has found international acceptance amongst international earthquake engineering communities. This pseudo-static analysis approach accounts for both hydrodynamic pressure and the inertial effects of mass concrete. This conventional "static" design approach has been widely employed to analysis concrete dams however in some cases, this method is based on unrealistic assumptions, and those dams designed according to this theory have experienced unacceptable damage during strong earthquakes. Meanwhile, in the current design approach, the linear elastic concept is taken into account in which the criteria of maximum principal stresses are implemented to vulnerability assessment of dams, where the non-linear behavior of mass concrete (damage-cracking) are ignored. Concrete, as a quasi-brittle material, behaves

Content from this work may be used under the terms of the Creative Commons Attribution 3.0 licence. Any further distribution of this work must maintain attribution to the author(s) and the title of the work, journal citation and DOI.
Published under licence by IOP Publishing Ltd

as linear elastic only when it is subjected to limited normal loads, while damage-cracking will occur as a result of tensile stresses exceed the concrete strength during strong earthquakes. Therefore, in the seismic vulnerability of large dams during the earthquake, it is necessary to evaluate the damage-cracking development in the dam body.

Seismic analysis of large dams has been the center of attention for researchers and dam's experts [2-7]. However, few, if any, researches have focused on the material nonlinearity of mass concrete, i.e. damage- cracking phenomenon [8]. Initial studies of material nonlinearity mainly consider fracture mechanics [9, 10], and the discrete crack model [9] to detect crack development in the mass concrete. As an alternative approach, the continuum method using the crack band model was also developed [11] to study the cracking of the concrete gravity dams, in which it takes into account the strain-softening characteristic of concrete. The crack band method labels the crack as a band comprising concentrated parallel fissures, whereas the material beyond the crack band remaining linear elastic[12]. This approach substitutes the orthotropic properties with isotropic constitutive relation within the failure zone. As soon as the concrete reaches its maximum tensile strength, the material located at the crack zone shows strain-softening performance and follows the equivalent softening constitutive relation.

In this paper, the seismic performance of an existing concrete arch dam was investigated considering damage-cracking development as a result of material nonlinearity under a strong earthquake. The plasticity-based five-parameter Willam-Warnke model [13] used for mass concrete and both cracking and crushing failure modes considered due to a multi-axial stress state. Besides, DCR (Demand Capacity Ratio) - CID (Cumulative Inelastic Duration) method was employed to evaluate the extent of the damage on the dam's body.

2. Research Methodology

2.1. Load Type and Combination

In the design of arch dams, it is essential to determine the loads required in the stability and stress analysis. In this study, the following loads were considered: Dead load, Water load (hydrostatic pressure), and hydrodynamic pressure due to Maximum Credible Level (MCL) ground motion. The dead load is calculated based on the weight of the concrete used in the construction of the dam body act on the center of gravity. The unit weight of concrete is generally assumed to be 24 KN/m^3.

The forces acting on arch dams due to water can be divided into two categories as hydrostatic and hydrodynamic Hydrostatic forces are static forces by the upstream water applied to arch dams. The magnitude of hydrostatic loads acting on arch dams can vary due to the rise or fall of the upstream during a flood or low rainfall months. Hydrodynamic forces are generally formed as a result of strong waves hitting to arch dams during extreme loading conditions i.e. an earthquake. The earthquake load consists of two types: inertia force due to the horizontal acceleration of the dam and hydrodynamic forces resulting from the interaction of the reservoir water and dam body.

During an earthquake, if the dam reservoir is filled with water, the distribution of the hydrodynamic forces can be calculated by Westergaard's theory. Then the hydrodynamic force is added to the hydrostatic force. In Westergaard's theory, it is possible to estimate the hydrodynamic forces at any water level of the dam reservoir.

$$F_{hd} = \gamma_\omega\,(\alpha)\;\; C_e\sqrt{H_u\, y} \tag{1}$$

F_{hd}, additional total water load down to depth y (Westergaard's theory), KN/m^2;
y, Depth from the reservoir water surface to the point of action of hydrodynamic pressure, (m);
C_e, factor depending principally on the depth of water and the earthquake vibration period T_e in second;

Westergaard's approximate equation for Ce, which is sufficiently accurate for all usual conditions calculated from the following equation:

$$C_e = \frac{0.9}{\sqrt{1 - 7(\frac{H_u}{1000\, T_e})^2}} \tag{2}$$

in which T_e is the period of the first mode.

According to the International Committee On Large Dams ICOLD [14], there are three seismic levels with different Peak Ground Acceleration (PGA) (Table 1). In the Design Basic Level (DBL), there is a possibility of a strong earthquake during the useful lifetime of the structure. At this level of shaking, the structure is assumed to resist lateral loading adequately without any structural damage. The percentage of risk-taking at this level is considered to be between 20 and 64%, for the useful lifetime of 100 years, and it is in proportion with the return period of 100 to 500 years. In the Maximum Design Level (MDL), the possibility of occurrence strong earthquake is low during the useful lifetime of the structure and it may experience damage to some extent; however, it should be able to continue operating. The percentage of risk at this level is between 10 and 20 %, which is in proportion with the return period of 500 to 1000 years. At the Maximum Credible Level (MCL), the structure is allowed to perform non-linearly. Damage to the structure might be severe, but these damages should be considered in the design process that guarantees reservoir safety without any human casualties in downstream. For many existing dams, the Construction Level (CL) with a return period of 50 years was considered at the time of project construction. In this research, MCL was taken into account to evaluate the hydrodynamic performance of the arch dam under consideration.

Table 1. Peak ground acceleration (PGA) for different seismic levels

Seismic design level	Return period (in years)	Maximum peak ground acceleration (g)	
		Horizontal (PGA H)	Vertical (PGA V)
CL	50	0.13g	
DBL	500	0.29 g	0.18 g
MDL	1000	0.39 g	0.27 g
MCL	Deterministic	0.54 g	0.44 g

In the MCL loading condition, the structure can have serious/un-repairable structural damages without the sudden release of the reservoir's water. Based on the previous reports provided [15], the most critical earthquake that the existing dams in MCL are exposed to, is the 1990 Manjil earthquake. Longitudinal components of Majil ground acceleration at MCL which was used in this analysis are shown in figure 1.

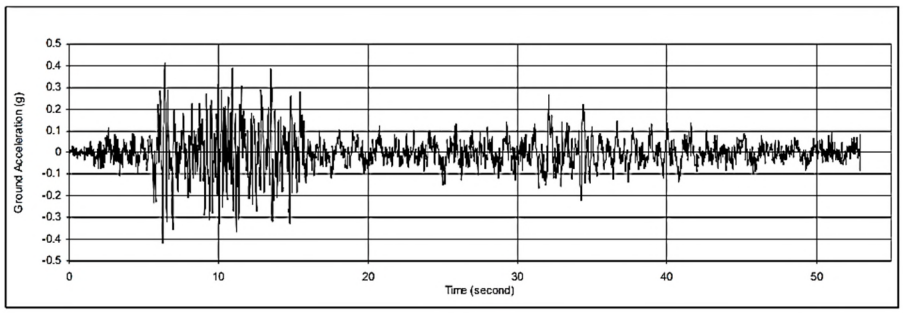

Figure. 1 Scaled acceleration for Manjil earthquake at Abbar station (Component L, MCL)

Table 2 shows the load combinations were considered in this study based on the ICOLD recommendation. To avoid analysis complexity, silt and thermal forces were not taken into account. Additionally, since the water was not directly modeled, the Westergaard theory was employed to simulate hydrodynamic forces. The earthquake force applied to the dam is proportional to the concrete mass.

Table 2. Load combinations

Load combination	Description
SU1	DL+Hs
SU2	DL+Hs+Hd
DU1	DL+Hs+Hd+E

DL is dead load, Hs is hydrostatic force, Hd is hydrodynamic force, and E is earthquake force

2.2. Material Properties

The modulus of elasticity, Poisson's ratio, and the unit weight are 40 GPa, 0.2, 24 KN/m^3 respectively for mass concrete. The actual compressive strength of concrete is assumed as 35 MPa. To calculate the tensile strength of concrete, the Raphael equation is used [16], equation (3), which states the true tensile strength of concrete which is close to the Brazilian test results [17].

$$f'_t = 0.34 {f'_c}^{2/3} = 3.4MPa \quad (3)$$

Table 3. summarizes the compressive and tensile stress, safety factors, and their relevant allowable stresses.

Table 3. compressive and tensile stress, safety factors, and relevant allowable stresses.

	Compressive stresses safety factor	Tensile stresses safety factor	Allowable compressive stresses (MPa)	Allowable tensile stresses (MPa)
Static condition	2	1	17.5	3.4
Dynamic condition	1.5	2	23.3	1.7

2.3. Failure Criterion

The Willam-Warnke model (plasticity-based five-parameter) was used for mass concrete failure criterion. Both crushing and cracking failure modes were taken into account. The criterion for mass concrete failure resulting from multi-axial stress state can be determined as follows:

$$\frac{\Omega}{f_c} - \gamma \geq 0 \quad (4)$$

where Ω is a function of the principal stress state, γ is the failure surface expressed in terms of principal stresses and the five input parameters which are described in Table 4.

Table 4. input parameters for failure criterion

Parameter	Description
f_t	Ultimate uniaxial tensile strength
f_c	Ultimate uniaxial compressive strength
f_{cb}	Ultimate biaxial compressive strength
f_1	Ultimate compressive strength for a state of biaxial compression superimposed on the hydrostatic stress state
f_2	Ultimate compressive strength for a state of uniaxial compression superimposed on the hydrostatic stress state

If equation (4) is satisfied, cracking or crushing of mass concrete occurs. In that case $_i f$ one of the principal concrete stresses is tensile, the crack occurs. On the other hand, if all principal stresses are compressive, crushing occurs. The failure surface can be specified with two parameters f_c and f_t. The other parameters in the Willam-Warnke model can be calculated by default as follows:

$$f_{cb} = 1.2\, f_c \quad (5)$$
$$f_1 = 1.45\, f_c \quad (6)$$
$$f_2 = 1.725\, f_c \quad (7)$$

However, these default values are valid only for stress states where the following condition is satisfied:

$$|\sigma_n| \leq \sqrt{3}\, f_c \qquad (8)$$
$$\sigma_n = \frac{1}{3}(\sigma_{xp} + \sigma_{yp} + \sigma_{zp})$$

Both function Ω and failure surface γ are expressed in terms of principal stresses denoted as σ_1, σ_2, and σ_3 where;

$\sigma_1 = \max(\sigma_{xp}\ ,\ \sigma_{xp}, \sigma_{xp})$ and $\sigma_3 = \min(\sigma_{xp}\ , \sigma_{xp}, \sigma_{xp})$ where $\sigma_1 \geq \sigma_2 \geq \sigma_3$

The failure of concrete is categorized into four domains:

$0 \geq \sigma_1 \geq \sigma_2 \geq \sigma_3$ (compression - compression - compression)
$\sigma_1 \geq 0 \geq \sigma_2 \geq \sigma_3$ (tensile - compression - compression)
$\sigma_1 \geq \sigma_2 \geq 0 \geq \sigma_3$ (tensile - tensile - compression)
$\sigma_1 \geq \sigma_2 \geq \sigma_3 \geq 0$ (tensile - tensile - tensile)

The general function Ω and the failure surface γ can be determined using independent relationships using concrete element consisting of the following assumptions and limitations:

i. Cracking at each Gaussian point in three orthogonal directions is allowed;
ii. If cracking occurs at a Gaussian point, the crack is modeled directly by modifying material properties;
iii. It is assumed that concrete is isotropic initially.

Cracking occurs when principal tensile stress in any direction lies outside the failure surface. In this model, cracking is permitted in three orthogonal directions at each Gaussian point. The presence of a crack at a Gaussian point and in a special direction represents through modification of stiffness matrix by exerting shear transfer coefficient in the cracked plane.

The reduction coefficient of tensile stress is assumed to be 0.6 in both static and dynamic conditions. In the utilized procedure, if the crack is closed, all compressive stresses orthogonal to crack plane can be transmitted and only a shear transfer coefficient βc ,in order to reduction of shear strength relative to the un-cracked case, is applied to the un-cracked matrix. The value of this parameter in the present study is equal to 0.9 for closed crack, and the strain-stress element matrix is as equation (9) that the superscript ck states that the strain-stress relationship is in the coordinate system parallel to the direction of principal stresses.

$$D_c^{ck} = \frac{E}{(1+\nu)(1-2\nu)} \begin{bmatrix} (1-\nu) & \nu & \nu & 0 & 0 & 0 \\ \nu & (1-\nu) & \nu & 0 & 0 & 0 \\ \nu & \nu & (1-\nu) & 0 & 0 & 0 \\ 0 & 0 & 0 & \frac{\beta_t(1-\nu)}{2} & 0 & 0 \\ 0 & 0 & 0 & 0 & \frac{1-2\nu}{2} & 0 \\ 0 & 0 & 0 & 0 & 0 & \frac{\beta_c(1-\nu)}{2} \end{bmatrix} \qquad (9)$$

It is worth noting that the relationship between β_t and $\beta_c$is always as follows:

$$0 < \beta_t < \beta_c < 1 \qquad (10)$$

In the present study, the value of the parameter β_t is taken as 0.2. Finally, the cracked element matrix is transferred to the element coordinate system by transfer matrix, $[T^{ck}]$, so that:

$$[D_c] = [T^{ck}][D_c^{ck}][T^{ck}] \qquad (11)$$

The above transfer matrix is a function of the crack strain of concrete. It is noticed that if at a point the concrete in the uni-axial, biaxial or tri-axial case is fractured, concrete is considered as crushed. At

this stage, the crushed element is eliminated from the stiffness matrix and its force is allocated to adjacent elements. Compressive stress-strain curvatures of concrete in dynamic conditions is shown in Figure 2.

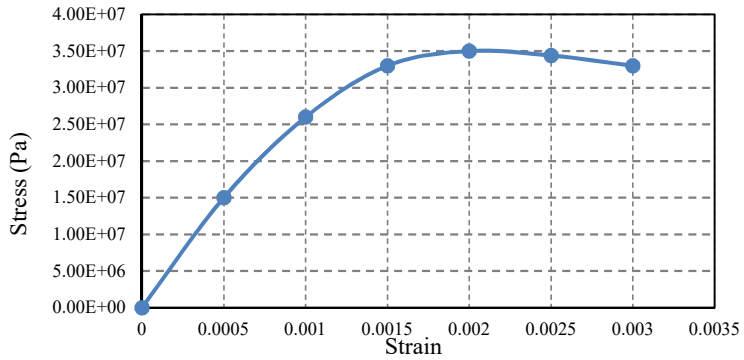

Figure. 2 Compressive stress-strain curve of concrete in dynamic conditions

2.4. Structural Damping

Structural damping is defined as a percentage of critical damping and is considered in the analysis as 5%. For the direct time integration, it is necessary to specify viscous damping in terms of Rayleigh damping with the mass and stiffness proportional to damping coefficients α_M and β_K, respectively. These parameters are chosen for two characteristic frequencies. The following relation between the damping ratio, the frequency and, the Rayleigh damping coefficients are used:

$$d = \frac{\alpha_M}{(2 \cdot \omega)} + \frac{\beta_K \cdot \omega}{2} \tag{12}$$

In the case of Rayleigh damping, it is only possible to obtain the desired damping at two frequencies. In this study, two frequencies were taken into account as 2 and 6 Hz. Accordingly, damping parameters based on equation 12 are: $\alpha_M = 0.94248\,\text{sec}$ and $\beta_K = 0.00199\ 1/sec$

3. Model Description

In the present study, a 30-meter height concrete arch dam having a cross-sectional thickness of 4 meters at the crest and 12 meters at foundation along with crest arch length of 62.83 meters was numerically investigated. The finite element model used for the structural analyses has been developed with the software SAP 2000.

4. Results and Discussion

4.1. Shape modes and displacement

The first four mode shapes of the dam are shown in figure 3 for full reservoir condition. The mode shape represents the characteristic dynamic oscillation of the structure for the respective eigenfrequency.

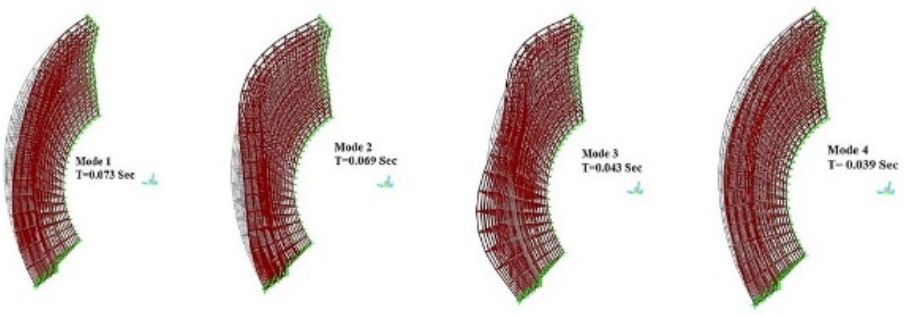

Figure. 3 The first four mode shapes of the case study

The result of Maximum crest displacement during Manjil MCL ground motion is shown in figure4. From figure 4, it can be observed that in the case of a dam with a rigid base, the maximum crest displacement is 1.8 cm.

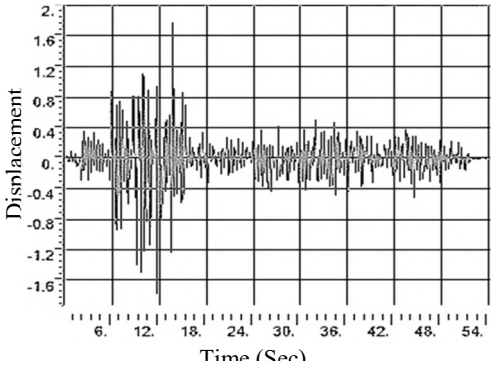

Figure. 4 Relative dynamic displacement of the crest (cm)

4.2. Principal stresses considering material nonlinearity at MCL level

In the following, the stresses are considered over the extent of the dam body. Tensile (+) and compressive (-) stresses are only reported in terms of principal stresses (Smax and Smin), while shear stresses represent the element shear in its local coordinates. For seismic load cases, the maximum and minimum principal stresses are taken from a critical time step during the analysis. Table 5 shows a summary of the absolute maximum or minimum value occurring in any node of upstream or downstream elements. These results are therefore indicative of extreme limits of the stress distributions.

Table. 5 Summary of stresses over dam body (in MPa)

	Upstream			Downstream		
Load Combination	SU1	SU2	DU1	SU1	SU2	DU1
Principal Compression	8	12.2	14	5.5	14.3	18.7
Principal Tension	2.3	3.5	4.4	1.8	2.4	3.8
Maximum Element Shear	3	0.9	1.05	2.7	0.4	1.3

The distribution of maximum principal stresses on the upstream and downstream faces of the dam at MCL level (time 10 sec) is shown in figure 5. A zone of high tensile stress, less than 4MPa, can be seen in the upstream face (upstream heel). Detailed consideration of the distribution of the maximum (tensile) principle stresses shows that the tensile stress developed in areas of the upstream face gradually reduces through the dam in the direction of the downstream face.

Overall, based on given results in Table 5, maximum compressive stress is about 19 MPa and remains well below the allowable compressive strength of the concrete for the extreme load scenario (allowable compressive stresses 32 MPa). However, high tensile stress exceeds the allowable tensile strength of the concrete, 1.7 MPa. The average tensile stress on the upstream face of the dam is around 4.0MPa with the maximum values occurring close to the (upstream heel) interface.

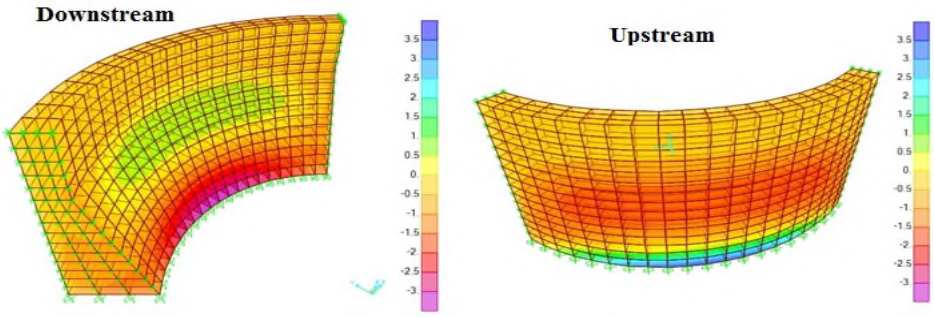

Figure. 5 Envelop values of Maximum Stresses at MCL level (time 10 sec)

Figure 6 shows the cracked Gaussian points on upstream faces at MCL considering material nonlinearity. Figure 6 shows that the most severely damaged region is in the bottom portion of the dam, where the cracks penetrate the small portion of the upstream heel with a maximum damage variable.

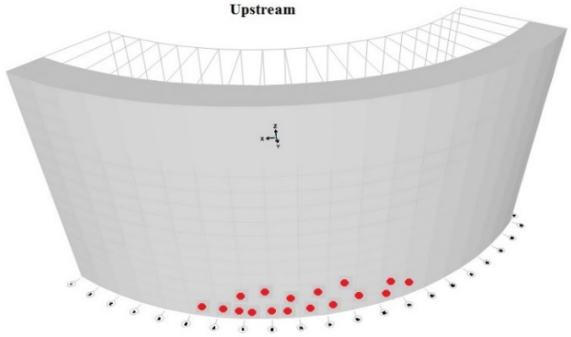

Figure. 6 Cracked Gaussian points

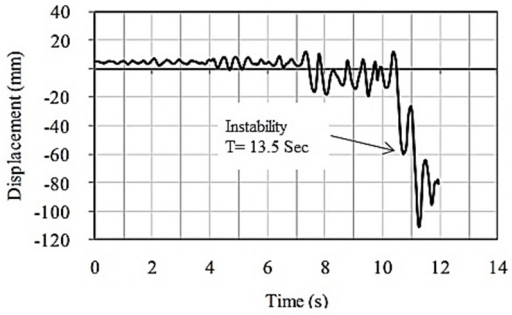

Figure. 7 Displacement time-history

In the present model, cracking starts about at the second 9th in the upstream face. In the second about 11, blocks perform almost separately and in 13.5s severe displacement is shown leads to the failure mechanism of the block as shown in figure 7. Considering the un-convergence of the block after 7 seconds of the beginning of earthquake loading, a significant displacement in the block leads to decide that dam is unsafe in the MCL earthquake.

4.3. Damage Evaluation using Demand Capacity Ratio- Cumulative Inelastic Duration

To assess dam stability under seismic events, the non-linear time-history method is used and is considered as one of the most reliable and prevalent methods of assessment. This method includes the DCR (Demand Capacity Ratio) - CID (Cumulative Inelastic Duration) method described in USACE Code [18]. According to this method, simple stress checks acquired from the non-linear analysis is used to assess the seismic performance of a dam. In general terms, in this method tensile stress should be lower than the allowable tensile strength of mass concrete. Nevertheless, a limited stress excursion beyond the allowable tensile strength is accepted for dynamic loadings. The performance evaluation and the assessment of damage level are expressed by relying on magnitudes of DCR, and cumulative duration of stress excursions beyond the tensile strength of the concrete and spatial extent of overstressed regions. Cumulative inelastic duration is roughly calculated by multiplying the number of stress excursions exceeding a certain DCR value by analytical time step. A performance curve presents the tolerable level of damage based on linear elastic analysis (Figure 8). The maximum allowable DCR for non-linear seismic analysis in large dams is 2. This value is equivalent to a stress demand twice the tensile strength of the concrete. in the proposed technique minor or no probability of damage can be

expected if the calculated DCR is lower than or equal to 1.0. The dam may experience nonlinear behavior in the form of cracking or opening of joints if the calculated DCR exceeds 1.0. The level of nonlinearity or concrete cracking assume low to moderate damage if the DCR is less than 2.0.

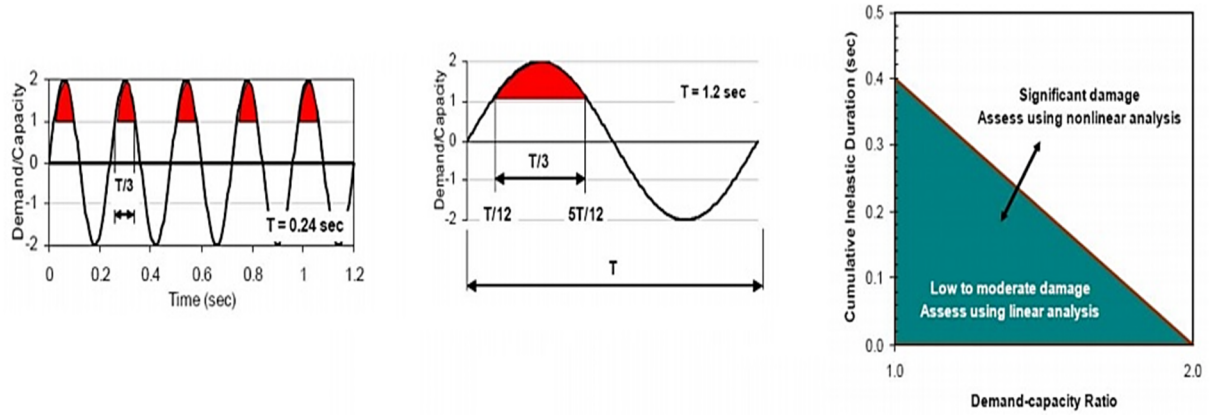

Figure. 8 Concept of Demand Capacity Ratio-Cumulative Inelastic Duration method [19]

Figure 9 shows that the performance curve due to the Manjil earthquake record where it is above the target line (in a limited area); demonstrates that the severe damages are occurred due to tensile stress.

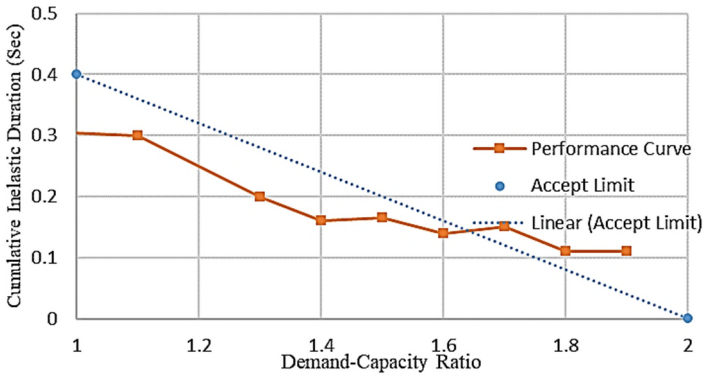

Figure. 9 Performance curve for case study subjected to Manjil earthquake

5. Conclusion

This study presents a seismic analysis of the arch concrete dam using non-linear time history analysis. The conclusions drawn from the above study are as follows:

i. The results show that seismic loading has a significant role in determining the final stress distribution within the dam body. In particular, the seismic load combinations appear to be more critical than those loads associated with the hydrostatic combinations.

ii. The maximum crest displacement was 18 mm when subjected to the MCL earthquake. Meanwhile, a band of high tensile stress is developed on the upstream face (upstream heel), with maximum values varying from about 3.5 MPa to about 4.4 MPa. As a result, cracks in the regions with high tensile stress could potentially be anticipated.

iii. The proposed material non-linearity failure criteria method predicted the crack patter adequately in conformity with principal stress distribution.

iv. The damage evaluation of the dam body was assessed utilizing a simplified demand capacity ratio- cumulative inelastic duration approach. The results indicated that the dam failed to address demand capacity ratio requirement and severe damages were expected as a result of high tensile stress.

References

[1] Han, R.P., *A simple and accurate added mass model for hydrodynamic fluid—Structure interaction analysis.* Journal of the Franklin Institute, 1996. **333**(6): p. 929-945.
[2] Hall, J.F. and A.K. Chopra, *Two-dimensional dynamic analysis of concrete gravity and embankment dams including hydrodynamic effects.* Earthquake Engineering & Structural Dynamics, 1982. **10**(2): p. 305-332.
[3] Calayir, Y. and M. Karaton, *Seismic fracture analysis of concrete gravity dams including dam–reservoir interaction.* Computers & structures, 2005. **83**(19-20): p. 1595-1606.
[4] Zhang, S. and G. Wang, *Effects of near-fault and far-fault ground motions on nonlinear dynamic response and seismic damage of concrete gravity dams.* Soil Dynamics and Earthquake Engineering, 2013. **53**: p. 217-229.
[5] Mirzabozorg, H., R. Kianoush, and M. Varmazyari, *Nonlinear behavior of concrete gravity dams and effect of input spatially variation.* Structural Engineering and Mechanics, 2010. **35**(3): p. 365-377.
[6] Sevim, B., A.C. Altunisik, and A. Bayraktar, *Structural identification of concrete arch dams by ambient vibration tests.* Advances in concrete construction, 2013. **1**(3): p. 227-237.
[7] Aminfar, M.H., et al., *Shape Optimization of Concrete Gravity Dams by ESO Method.* World Applied Sciences Journal, 2008. **5**(6): p. 675-679.
[8] Azmi, M. and P. Paultre, *Three-dimensional analysis of concrete dams including contraction joint non-linearity.* Engineering Structures, 2002. **24**(6): p. 757-771.
[9] Ayari, M.L. and V.E. Saouma, *A fracture mechanics based seismic analysis of concrete gravity dams using discrete cracks.* Engineering Fracture Mechanics, 1990. **35**(1-3): p. 587-598.
[10] Lee, J. and G.L. Fenves, *A plastic-damage concrete model for earthquake analysis of dams.* Earthquake engineering & structural dynamics, 1998. **27**(9): p. 937-956.
[11] Calayir, Y. and M. Karaton, *A continuum damage concrete model for earthquake analysis of concrete gravity dam–reservoir systems.* Soil Dynamics and Earthquake Engineering, 2005. **25**(11): p. 857-869.
[12] Bažant, Z.P. and B.H. Oh, *Crack band theory for fracture of concrete.* Matériaux et construction, 1983. **16**(3): p. 155-177.
[13] Hariri-Ardebili, M., S. Seyed-Kolbadi, and M. Kianoush, *FEM-based parametric analysis of a typical gravity dam considering input excitation mechanism.* Soil Dynamics and Earthquake Engineering, 2016. **84**: p. 22-43.
[14] Dams, T.I.C.o.L., *International Commission on Large Dams*. 2018.
[15] Hariri-Ardebili, M. and S. Seyed-Kolbadi, *Seismic cracking and instability of concrete dams: Smeared crack approach.* Engineering Failure Analysis, 2015. **52**: p. 45-60.
[16] Ahmed, M., J. Mallick, and M.A. Hasan, *A study of factors affecting the flexural tensile strength of concrete.* Journal of King Saud University-Engineering Sciences, 2016. **28**(2): p. 147-156.
[17] *López*, C.M., I. Carol, and A. Aguado, *Meso-structural study of concrete fracture using interface elements. II: compression, biaxial and Brazilian test.* Materials and structures, 2008. **41**(3): p. 601-620.
[18] *Hariri*-Ardebili, M. and V. Saouma, *Collapse fragility curves for concrete dams: comprehensive study.* Journal of Structural Engineering, 2016. **142**(10): p. 04016075.
[19] *Wang*, G., et al., *Integrated duration effects on seismic performance of concrete gravity dams using linear and nonlinear evaluation methods.* Soil dynamics and earthquake engineering, 2015. **79**: p. 223-236.